ACS APPLIED MATERIALS & INTERFACES

Research Article

www.acsami.org

Conjugation-Grafted-TiO_2 Nanohybrid for High Photocatalytic Efficiency under Visible Light

Ping Lei,[†] Feng Wang,*[,†] Shimin Zhang,[†] Yanfen Ding,[†] Jincai Zhao,[‡] and Mingshu Yang*[,†]

[†]Beijing National Laboratory for Molecular Sciences, Key Laboratory of Engineering Plastics, Institute of Chemistry, and [‡]Key Laboratory of Photochemistry, Institute of Chemistry,Chinese Academy of Sciences, Beijing 100190, P. R. China

Supporting Information

ABSTRACT: Abundant and renewable solar light is an ideal resource for the industrial application of TiO_2 photocatalysis in environmental purification. Over the past decades, the pursuit for visible-light photocatalysts with low cost, simple process, and high efficiency remains a challenging task. Here, we report a novel organic−inorganic nanohybrid photocatalyst (conjugation-grafted-TiO_2) by chemically grafting conjugated structures onto the surfaces of TiO_2 nanoparticles through controlled thermal degradation of the coacervated polymer layer. The interfacial C−O−Ti bonds between TiO_2 and conjugated structures can act as the pathway to quickly transfer the excited electrons from conjugated structures to TiO_2, therefore contribute to high visible-light photocatalytic efficiency. Our findings provide an economic route to prepare the conjugation-grafted-TiO_2 nanohybrid, and develop a routine to improve the photocatalytic efficiency of organic−inorganic hybrid materials through the interfacial interaction.

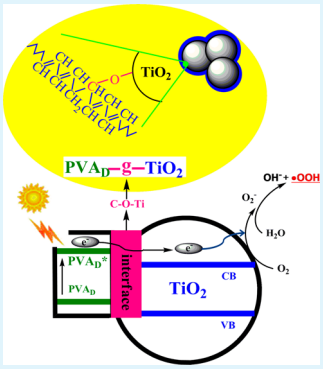

KEYWORDS: *electron transfer, visible light, TiO_2, nanohybrid, conjugation, grafting*

INTRODUCTION

Since the success of hydrogen production through titanium dioxide (TiO_2) photocatalytic water-splitting by Fujishima and Honda in 1972,[1] TiO_2 photocatalysis has attracted great attention in view of its applications to solar energy conversion, hydrogen production, self-cleaning surface, and air and water purification.[2] However, its practical applications have been limited because of a serious drawback that TiO_2 photocatalyst can only absorb ultraviolet light (UV accounts for only 3% of the incoming solar energy) to photocatalytic reactions.[3] Extensive efforts have been devoted to developing visible-light (VL)-driven TiO_2-based photocatalysts for using abundant and green sunlight.[4] An effective strategy is to modify the surface of TiO_2 with VL-absorbing conjugated materials.[5−8] Conjugated materials, with the extending π-conjugated electron system, are efficient electron donors and good hole transporters.[7,9] In conjugation/TiO_2 system, conjugated materials can harvest VL to be excited and then inject the excited electrons into the conduction band of TiO_2.[9,10] Nevertheless, to date, these conjugated materials have typically suffered from high cost, complex preparation process, and easy loss from the surface of TiO_2. Therefore, to exploit a stable conjugation/TiO_2 photocatalyst using a simple and cheap method would be desirable.

Apart from synthesis method, conjugated materials could also be easily obtained from polymer degradation. There is such a class of polymers that their main molecular chains are saturated and has side group, such as polyvinyl alcohol (PVA), polyvinyl chloride (PVC), polystyrene (PS), etc. Under heat-treatment, the degradation of these polymers occurs based on elimination of side groups from the main chain to form conjugated structure. Some researchers[11−13] treated the TiO_2/polymer mixture at high temperature to induce polymer degradation and form conjugated structures on the surface of TiO_2. In such materials, controlling the interfacial interaction between the conjugated structures and TiO_2 is crucial and indispensable. It is well-known that the electron transfer on the interface between the conjugation and TiO_2 is of great significance to the photocatalytic efficiency.[14,15] The strong interaction could accelerate the electron transfer on the interface, then cause a rapid photoinduced charge separation and a relatively slow charge recombination, and hence improve the photocatalytic efficiency.[16,17] Although these polymers have been used to prepared VL-driven photocatalyst, the interaction between TiO_2 photocatalyst and the conjugated structures from polymer degradation has been rarely studied, especially the direct chemical bonding.

Herein, we designed a simple route of coacervation combined with controlled degradation to fabricate a chemically bonded conjugation-grafted-TiO_2 nanohybrid photocatalyst with inexpensive PVA and TiO_2 (P25). Under the role of heat, the PVA molecular chains coacervated on the surface of TiO_2 degraded to form conjugated structures and attached onto the surface of TiO_2 via the interfacial C−O−Ti bonds between PVA and TiO_2. Most importantly, the interfacial C−O−Ti bonds can act as the electron transfer pathway to accelerate the excited electrons transferring from conjugation structures to

Received: October 21, 2013
Accepted: January 13, 2014
Published: January 14, 2014

   dx.doi.org/10.1021/am4046537 | ACS Appl. Mater. Interfaces 2014, 6, 2370−2376

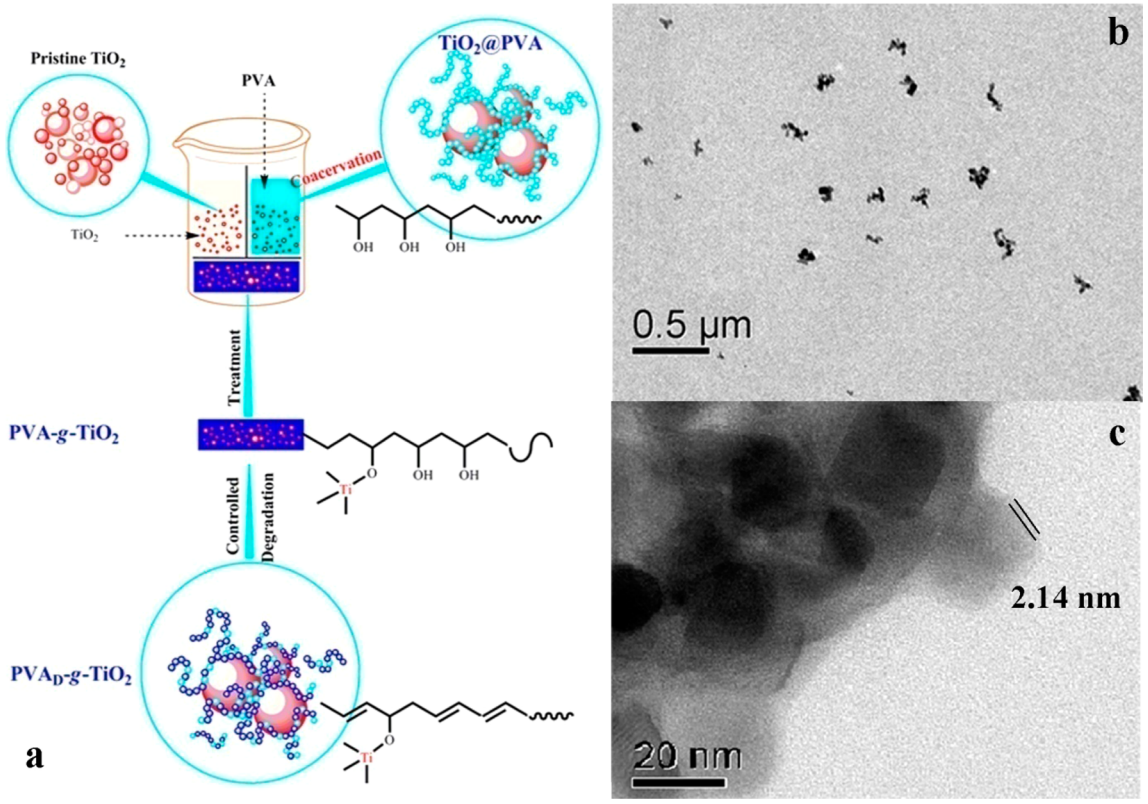

Figure 1. (a) Schematic illustration for the fabrication process of the PVA_D-g-TiO_2 (C-g-T) nanohybrid. (b) TEM image and (c) HR-TEM image of the C-g-T nanohybrid obtained at 220 °C with TiO_2/PVA weight ratio of 20:1.

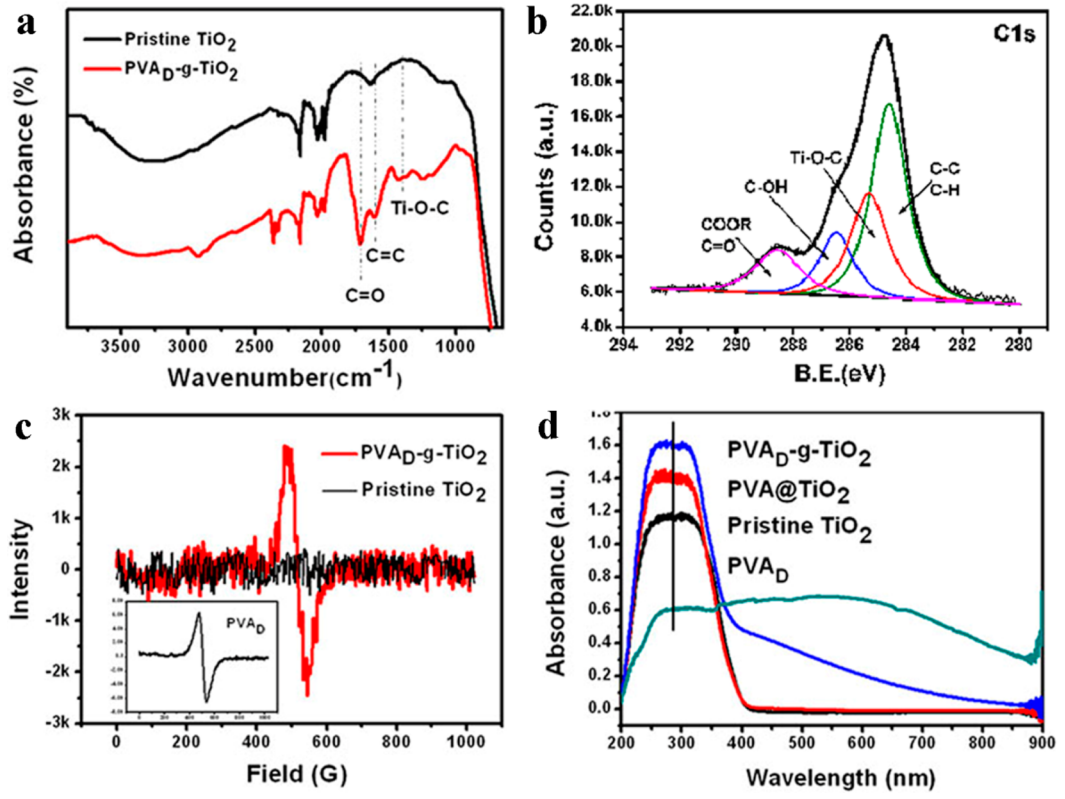

Figure 2. (a) ATR-FTIR, (b) C1s XPS, (c) EPR, and (d) UV−vis DRS spectra of PVA_D-g-TiO_2 (C-g-T) nanohybrid obtained at 220 °C with TiO_2/PVA weight ratio of 20:1 in comparison with pristine TiO_2 and others.

dx.doi.org/10.1021/am4046537 | ACS Appl. Mater. Interfaces 2014, 6, 2370−2376

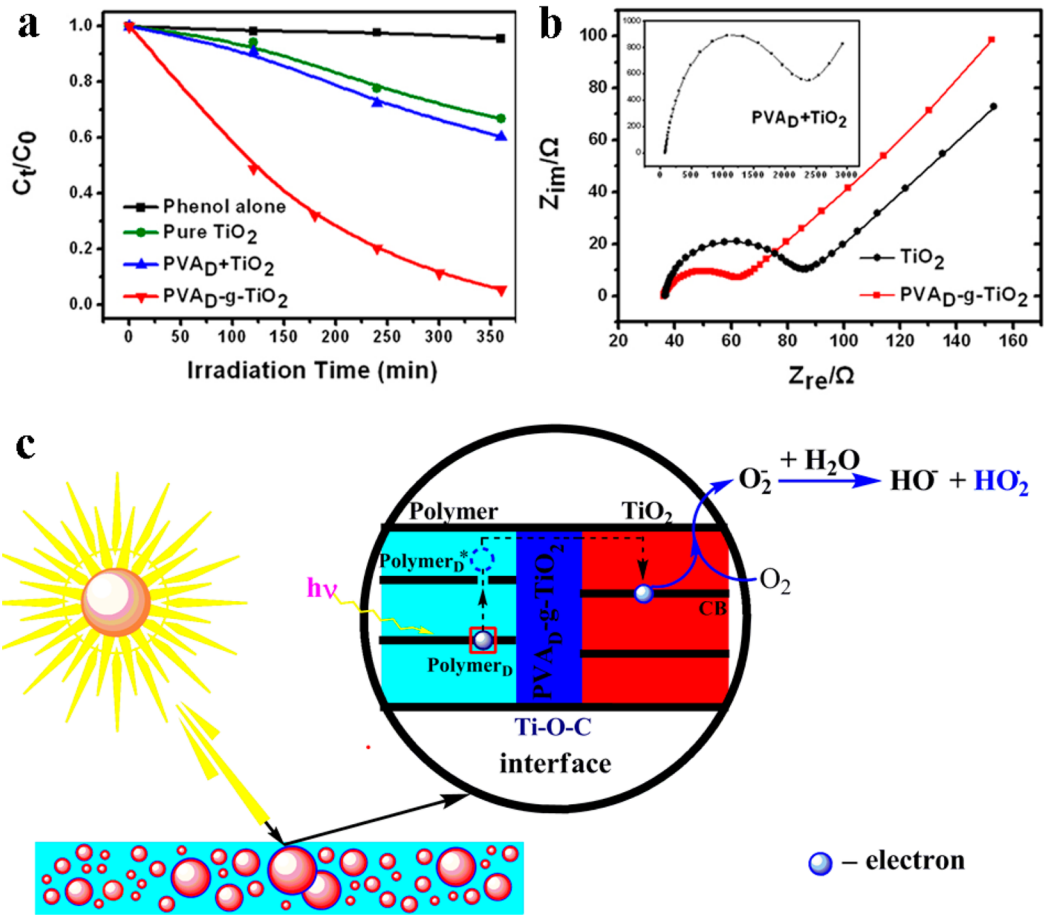

Figure 3. Electron transfer in the interface of PVA_D-g-TiO_2 (C-g-T) nanohybrid. (a) Photocatalytic degradation of phenol by C-g-T nanohybrid and others under VL irradiation (λ > 450 nm). (b) EIS changes of pristine TiO_2, C-g-T nanohybrid, and PVA_D+TiO_2 mixture (inset). PVA_D+TiO_2 mixture has the same weight of TiO_2 and PVA_D with C-g-T nanohybrid. (c) Possible charge separation and transfer mechanism of C-g-T nanohybrid under VL irradiation.

TiO_2, and hence significantly improve the photocatalytic efficiency of the nanohybrid photocatalyst. The results demonstrated in this work should give a useful enlightenment for the design of more efficiency and practical TiO_2-based VL-induced photocatalyst.

RESULTS AND DISCUSSIONS

Formation of Conjugation-Grafted-TiO_2 Nanohybrid. The conjugation-grafted-TiO_2 nanohybrid is simply fabricated by the route shown in Figure 1a. At first, to obtain homogeneous polymer-encapsulated nanoparticles, coacervation method is utilized to prepare TiO_2@PVA precursor via the theory of phase separation.[18−20] By this method, quantified PVA molecules can be uniformly coated on the surfaces of TiO_2 nanoparticles, superior to the traditional physical mixing, polymerization and hydrothermal methods. The TiO_2@PVA precursor is then thermally treated at high temperature. During this process, PVA molecules are attached onto TiO_2 nanoparticles via C−O−Ti bonds, and then different lengths of carbon−carbon conjugated chains are formed through the controlled degradation of PVA molecules (PVA_D). The final PVA_D-g-TiO_2 nanohybrid is denoted as conjugation-grafted-TiO_2 (C-g-T in abbreviation).

As shown in Figure 1b, the C-g-T nanohybrid is dispersed in the form of small aggregates with a smaller size of 50−100 nm than the pristine TiO_2 nanoparticle aggregates (see Figure S1 in the Supporting Information). To visualize the conjugated PVA_D layer coated on the surface of TiO_2, high-resolution TEM (HRTEM) is further used (Figure 1c). It is obvious that a clear PVA_D layer is uniformly wrapped on the surface of TiO_2 aggregate with an average thickness of about 2.14 nm, but is absent for the pristine TiO_2 nanoparticles (see Figure S2 in the Supporting Information). Furthermore, a new signal of C (Kα) appears in the energy dispersive X-ray (EDX) spectroscopy of the C-g-T nanohybrid (see Figure S3 in the Supporting Information). X−ray diffraction (XRD) patterns displayed in Figure S4 show the same characteristic peaks of C-g-T nanohybrid as the pristine TiO_2, which indicates that the crystalline form of TiO_2 nanoparticles remains unchanged during the heat treatment.

More detailed information regarding the chemical structure of the C-g-T nanohybrid is characterized by Attenuated Total Reflectance/Fourier transform infrared spectrometry (ATR/FTIR) and X-ray photoelectron spectroscopy (XPS). Figure 2a presents the ATR spectra of the C-g-T nanohybrid in comparison with the pristine TiO_2. The new characteristic absorption at 1715 cm^{-1} and 1602 cm^{-1} are attributed to the −C═O bond stretching and −C═C− conjugated bond stretching, respectively. In addition, the peak at 1261 cm^{-1} is assigned to the vibration of C−O−Ti bonds between the PVA_D and TiO_2 nanoparticles.[21] These results are further confirmed by XPS (Figure 2b). The high−resolution XPS spectrum of

dx.doi.org/10.1021/am4046537 | ACS Appl. Mater. Interfaces 2014, 6, 2370−2376

C1s for C-g-T is resolved into three Gaussian curve−fitted peaks: −C═O around 288.5 eV, C−O−Ti around 285.95 eV[22] and −C═C− around 284.76 eV from high to low binding energy, respectively. In Ti2p XPS, the characteristic peak of C−O−Ti appears at 460.95 eV (see Figure S5 in the Supporting Information).

Electron paramagnetic resonance (EPR) is a widely used probe to detect the unpaired electrons on π-conjugated materials.[23] In Figure 2c, a Lorentzian line is observed for C-g-T nanohybrid but absent for the pristine TiO_2. This confirms the formation of π-conjugated structures on the surfaces of TiO_2 in C-g-T nanohybrid, which is attributed to the delocalized $\pi-\pi^*$ electrons of the large carbon−carbon conjugated chains formed in the PVA_D layer (the inset in Figure 2c) attached on the surface of TiO_2. Moreover, the absorption range of light plays an important role in photocatalysis, especially for the VL photodegradation of pollutants.[24] UV−vis diffuse reflectance spectra (UV−vis DRS) is used to study the optical properties of C-g-T nanohybrid compared with other reference samples (Figure 2d). The analysis shows that C-g-T nanohybrid has a broad absorption in VL regions, which is ascribed to the $\pi-\pi^*$ transition of the carbon−carbon conjugated chains in the outer PVA_D layer. The width of absorption band in VL region indicates the coexistence of both long and short effective conjugation lengths in the conjugated chains,[7] beneficial to increasing the light harvest. Based on above results, it is concluded that the solar spectrum can be used for effectively driving photocatalytic reactions with the C-g-T nanohybrid.

The above evidence lead to the following conclusions. During the heating process, the active −OH groups on the surface of TiO_2 begin to react with the −OH groups in PVA molecular chains through dehydration reaction. Meanwhile, the PVA molecules grafted onto the surface of TiO_2 degrade to generate −C═O and −C═C− groups, and the various adjacent −C═C− groups constitute different lengths of carbon−carbon conjugated chains. Therefore, the conjugated chains could be grafted firmly onto the TiO_2 surfaces through C−O−Ti bonds and finally the chemically bonded C-g-T nanohybrid is obtained.

Stability of the nanohybrid catalyst is of great importance for the practical application in wastewater treatment. In the C-g-T nanohybrid, there are C−O−Ti bonds formed during the thermal degradation the PVA/TiO_2 precursor and thus the two components are combined firmly and expected to have good stability after photocatalytic reactions.The grafted PVA_D lose in the 20:1 C-g-T hybrid after photodegradation cycles was tested through the following procedures: At the end of each cycle, the reaction admixture was centrifuged at 10 000 rpm for 10 min, and the precipitating was recycled and used for the next cycle of the photodegradation test. After five cycles of photodegradation test, the solid recovered from the testing admixture was leached carefully and dried. Compared with the initial thermogravimetric residue of nanohybrid 95.7 wt %, the thermogravimetric residue of PVA_D-g-TiO_2 after five cycles was 95.9 wt %, which suggests that most of the grafted PVA_D did not loss from the surface of TiO_2 after several runnings of degradation test.

Efficient Charge Transfer on C-g-T Nanohybrid. The above-mentioned results have confirmed that the conjugated PVA_D is strongly grafted onto the surface of TiO_2 by C−O−Ti bonds. We propose that the C−O−Ti bonds can act as the pathway to quickly transfer the excited electrons from PVA_D to TiO_2. It is well-known that the rapid charge transfer can achieve an effective charge separation, therefore contributes to high photocatalytic efficiency. To test whether the electron transfer is achieved through the interfacial C−O−Ti bonds between TiO_2 and PVA_D, we compare the photocatalytic activity of the chemically bonded PVA_D-g-TiO_2 with an equivalent physical mixture of TiO_2 and PVA_D (PVA_D+TiO_2) (see Experimental Methods section). Figure 3a illustrates the time profile of the degradation of phenol in suspensions of PVA_D-g-TiO_2, PVA_D+TiO_2 and pristine TiO_2 under VL irradiation. Upon the VL irradiation, phenol is very stable in the aqueous solution, revealing almost unchanged concentration. The PVA_D-g-TiO_2 nanohybrid shows the highest photocatalytic efficiency by ca. 95% reduction of the initial phenol concentration after the 360 min VL irradiation, whereas the PVA_D+TiO_2 mixture is much less active (~40% reduction), few superior to the pristine TiO_2 (~33% reduction). The marked difference between PVA_D-g-TiO_2 and PVA_D+TiO_2 indicates that the interfacial C−O−Ti chemical bonds in PVA_D-g-TiO_2 act as the electron transfer pathway and thus improve the photocatalytic efficiency. Additionally, degradation test to MO and formaldehyde solution showed the similar activity in Figure S7 in the Supporting Information, which suggested that visible-light photocatalysis of PVA_D-g-TiO_2 was not based on the dye-sensitization but on the grafted conjugation.

To obtain further insight to the photocatalytic mechanism of the C-g-T nanohybrid, we investigated the charge separation and transfer from conjugated PVA_D to TiO_2, which is of critical importance to the photocatalytic efficiency of C-g-T nanohybrid. Electrochemical impedance spectroscopy (EIS) is applied as an additional characterization tool to distinguish the interfacial structure of the modified nanoparticles.[25] The semicircle portion in EIS spectrum represents the electron-transfer-limited process, and the semicircle diameter equals the electron-transfer resistance, R_{et}.[25,26] Figure 3b compares the Nyquist plots of EIS observed upon pristine TiO_2, physical mixing PVA_D+TiO_2, and chemical bonded PVA_D-g-TiO_2. After the attachment with conjugated PVA_D, though in small amount, the semicircle in the plot of PVA_D-g-TiO_2 shows the smallest semicircle, which indicates a decrease in the solid state interface layer resistance and R_{et} value on the surface.[27,28] Because of its delocalized π-conjugated electron system, conjugated PVA_D has excellent conductivity. Meanwhile, the interfacial C−O−Ti bonds can act as the fast pathway, which accelerates the electron transfer from the conjugated PVA_D chains to the conduction band of TiO_2 during photocatalysis.

On the basis of the above discussion, the mechanism of electron transfer process between PVA_D and TiO_2 in the C-g-T nanohybrid can be illustrated in Figure 3c. For C-g-T, the conjugated PVA_D molecules instead of TiO_2 photocatalyst, are excited by VL irradiation. The excited delocalized π-electrons in the ground state of PVA_D are injected to the conduction band of TiO_2 through the interfacial pathway of C−O−Ti bonds, whereas the PVA_D itself is converted to its cationic radical of PVA_D*. Then, the injected electrons subsequently migrate to the edge of TiO_2 and react with the dioxygen adsorbed on the surface of TiO_2 to generate a series of active oxygen species such as $O^{2\cdot-}$, ·OH and H_2O_2.[7,11,29] The subsequent oxidative and reductive reactions lead to the degradation of the organic pollutants. In this process, the conjugated PVA_D chains act as electron donors, whereas the conduction band of TiO_2 nanoparticles act as electron acceptors. The well-bridged interfaces composed of C−O−Ti bonds allow the electrons to rapidly migrate from PVA_D to TiO_2, and reduce the

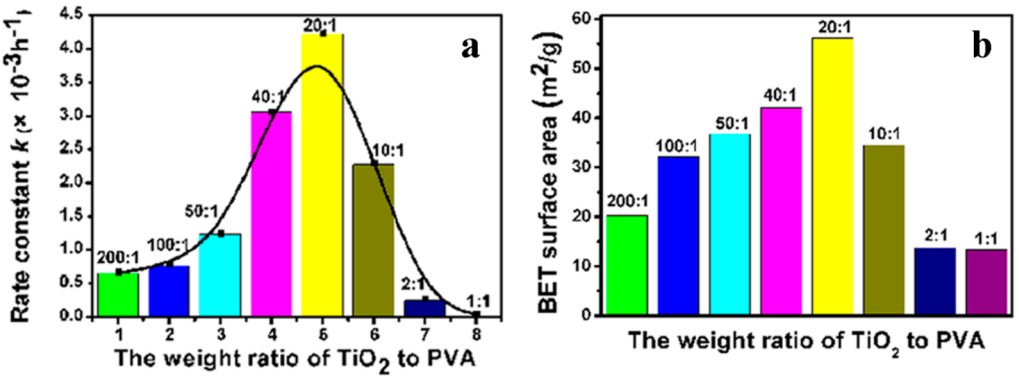

Figure 4. Influence of the weight ratio of TiO_2/PVA on (a) the rate constant k under visible light ($\lambda > 450$ nm) and (b) the BET specific surface areas of the C-g-T nanohybrids prepared at 140 °C with different TiO_2/PVA weight ratio.

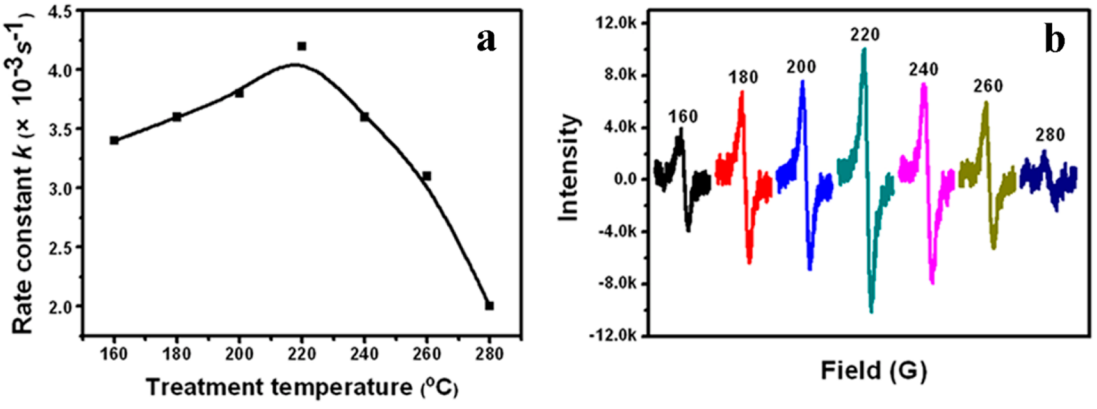

Figure 5. Influence of the degradation temperature on a) the rate constant k under visible light ($\lambda > 450$ nm) and (b) the EPR spectra of the C-g-T nanohybrids prepared at different temperature with the same TiO_2/PVA weight ratio of 20:1.

probability of electron−hole (e^-−h^+) pair recombination. Therefore, C−O−Ti chemical bonds between PVA_D molecules and TiO_2 nanoparticles are critical to the superior photocatalytic activity of C-g-T nanohybrid. During the step of the pollutants' degradation, unexcited electrons are produced and transfer to PVA_D to compensate the migration of the exited electrons to TiO_2, completing an electron recycling.

Optimization of C-g-T Nanohybrid Photocatalyst. To obtain the highly efficient and well-controlled C-g-T nanohybrid photocatalysts, we investigated the effects of TiO_2/PVA weight ratio and degradation temperature on photocatalytic efficiency, respectively.

A series of TiO_2@PVA precursors with various PVA additions are prepared and then thermal degraded at the temperature of 220 °C. The TGA results confirm that the TiO_2/PVA ratios are in good agreement with the predetermined values (see Table S1 in the Supporting Information). It implies that, in the process of coacervation, the added PVA is completely coacervated on the surfaces of TiO_2 nanoparticles. The resultant C-g-T nanohybrids are applied to degrade methyl orange (MO) under VL irradiation, and the degradation rate constant (k) is calculated (see the Supporting Information). It is clearly illustrated in Figure 4a that the rate constant increases at first and then decreases with the increase in PVA addition (decreasing TiO_2/PVA weight ratio). The result uncovers that TiO_2/PVA weight ratio is a key factor to obtain optimal photocatalytic efficiency. It is noticeable that the TiO_2/PVA weight ratio has something to do with both the surface area and the content of PVA_D, which are vital to the photocatalytic efficiency. Generally, a higher surface area means more active sites available for trapping charge carriers and adsorbing reactant species.[30,31] Meanwhile, more PVA_D can provide larger amount of conjugated structures to harvest VL. Nevertheless, excess PVA_D may be disadvantageous to the surface area of the samples.[31] Therefore, it is important to maintain a balance between the content of PVA_D and the surface area by adjusting the TiO_2/PVA weight ratio.

BET surface area illustrated in Figure 4b shows the same trend as the effect on photocatalytic efficiency in Figure 4a. In the region of the weight ratio decreasing from 200:1 to 20:1, the coacervated PVA molecules on the surfaces of TiO_2 help to reduce the polarity of TiO_2 nanoparticles and improve the dispersion of the samples; meanwhile, the higher PVA content contributes to the more conjugated structures in samples. As a result, the photocatalytic efficiency enhances with the increase in PVA addition. When the weight ratio decreases to 20:1, the photocatalyst has the largest BET surface area of 56.3 m^2/g and results in the highest photocatalytic efficiency (shown in Figure 4a). Nevertheless, the BET surface area quickly reduces with the weight ratio decreasing from 20:1 to 1:1, leading to the decreased photocatalytic efficiency. Furthermore, the TEM images (see Figure S6 in the Supporting Information) present that the excess PVA molecules further wrap the PVA@TiO_2 precursor to form severe aggregates, which greatly reduces the surface area and is disadvantageous for the adsorption and photocatalytic degradation.[30] Therefore, it can be concluded that the effect of TiO_2/PVA weight ratio on surface area of the samples is the dominant factor for photocatalytic efficiency.

dx.doi.org/10.1021/am4046537 | ACS Appl. Mater. Interfaces 2014, 6, 2370−2376

To illustrate the relationship between the degradation temperature and the photocatalytic efficiency, PVA@TiO_2 precursor with the TiO_2/PVA weight ratio of 20:1 is degraded at different temperature. The rate constant (k) of MO degradation by the resultant C-g-T samples is calculated and shown in Figure 5a. With an increasing temperature, the rate constant first increases and then decreases, and the sample treated at 220 °C exhibits the highest efficiency. The difference in the photocatalytic efficiency of these samples is reasonably ascribed to the various contents of $\pi-\pi^*$ conjugated structures in PVA_D from the degradation of PVA under various temperature. Temperature is a major factor on PVA degradation as well as the formation of the conjugated structure.

To further study the effect of the degradation temperature on the formation of conjugated structures, EPR spectra of the samples are also obtained. Generally, this Lorentzian line can be greatly enhanced after the formation of heterostructure, presumably due to the redistribution of π electrons within heterojunction by band offsets.[32] Thus, the intensity of EPR response contributes to the amount of delocalized π-conjugated electrons in the conjugated PVA_D layer. As presented in Figure 5b, the intensity of EPR response of the C-g-T nanohybrids against degradation temperature shows the same tendency compared with the curve of rate constant against degradation temperature. The strongest response is observed for the sample treated at 220 °C, the temperature at which the thermal degradation of PVA molecules tend to form more conjugated C═C groups in the C-g-T nanohybrid. As mentioned above, the highest photocatalytic efficiency is achieved for the C-g-T nanohybrid from PVA@TiO_2 degraded at 220 °C, which can be explained as follows. The conjugated PVA_D layer on the surface of TiO_2, acting as the sensitizer, can harvest the VL and accelerate the separation of the photogenerated electrons and holes.[33] Therefore, the C-g-T nanohybrid possesses photocatalytic activity under VL irradiation. The absorption ability of the photocatalyst for VL is one of the crucial factors in photocatalysis. The more conjugated structures in PVA_D lead to the higher photocatalytic efficiency and so far the C-g-T nanohybrid from PVA@TiO_2 degraded at 220 °C. It is concluded that the root cause of the effect of degradation temperature on photocatalytic efficiency ascribes to its effect on the formation of conjugated chains on the surface of TiO_2.

CONCLUSION

In summary, we have developed a facile method to prepare a chemically bonded conjugated-grafted-TiO_2 nanohybrid via polymer degradation onto the surface of TiO_2 nanoparticles. The C-g-T nanohybrid shows high efficiency in photodegradation of organic compounds under VL irradiation. This is attributed to both the effective VL harvest by the conjugated structures in degraded polymer layer and the efficient electron transfer through the C−O−Ti bonds between TiO_2 and conjugated structures. We find that the weight ratio of 20:1 (TiO_2/PVA) and heat treatment of 220 °C are the suitable preparation conditions for the higher photocatalytic efficiency. This novel design of C-g-T nanohybrid is a promising method to fabricate VL-driven TiO_2-based photocatalyst and facilitate their practical application in the environmental protection.

EXPERIMENTAL METHODS

Preparation of PVA_D-g-TiO_2 Nanohybrid. Pristine TiO_2 nanoparticles were initially dispersed in deionized water. The mixture was stirred for another 1 h to reach a uniform TiO_2 suspension system. PVA aqueous solution was subsequently added into the suspension, followed by mechanical stirring for 0.5 h. After that, ethanol, as the nonsolvent of PVA, was dropped slowly through a constant pressure funnel. With the dropping of ethanol, the phase separation occurred and initiated the coacervation of PVA on the surface of TiO_2 to form PVA@TiO_2 precursor. The PVA@TiO_2 precursor was collected by filtration and washed several times with absolute ethanol to wipe off the extra PVA, and then was dried for a week under room temperature. Afterward, the dried particles were grinded in a mortar box, and subsequently heat-treated at different temperature for 2 h in a muffle. The resulting sample particles were referred as PVA_D-g-TiO_2 (C-g-T in abbreviation). In addition, for comparison purpose, pure PVA was also heat-treated at 220 °C for 2 h and the resulting sample was referred as PVA_D. The PVA_D+TiO_2 mixture was prepared by mechanical mixing the pristine TiO_2 with PVA_D.

Characterization. The as-prepared PVA_D-g-TiO_2 (C-g-T) photocatalysts were transferred onto different substrates for the measurements of SEM (Hitachi, S-4300), TEM (JEOL JEM-2010), X-ray diffraction (XRD, Japan, Rigaku D/max-2500), FTIR/ATR (Thermo Nicolet 6700 FTIR), UV−visible DRS (TU−1901, Pgener al), X-ray photoelectron spectra (XPS, VG Scientific, ESCALab220i-XL), BET surface area (ASAP 2010), electron paramagnetic resonance (EPR, Bruker, ESP300E), and electrochemical impedance spectroscopy (EIS, Germany, Zahner, Zennium).

Photocatalytic Degradation Test. Photocatalytic activity of the as-prepared nanohybrid photocatalysts was evaluated from the degradation rate of methyl orange (MO, $(H_3C)_2NC_6H_4N_2C_6H_4SO_3Na$) and phenol ($C_6H_5OH$) in an aqueous solution with an initial concentration of 15 mg/L and 10 mg/L, respectively. The sample photocatalyst containing 10 mg TiO_2 was dispersed in 10 mL MO or phenol solution by stirring under irradiation. The photocatalysis reaction was carried out in a photochemical reactor. The visible light source was a 500 W halogen lamp put in a cylindrical glass vessel with a recycling water glass jacket; meanwhile, a cutoff filter was placed outside the water jacket to completely remove any radiation at wavelengths below 450 nm, thereby ensuring illumination by visible light only. Prior to irradiation, the suspensions were magnetically stirred in the dark for 1 h to establish an adsorption−desorption equilibrium. The adsorption of MO was found to be very little and could be neglected compared with the change of concentration of MO under photocatalysis. At given time intervals, 5 mL of suspension was centrifuged and the upper solution was sampled for analysis. In addition, for the purpose of comparison, pristine TiO_2 and physical mixing PVA_D+TiO_2 were also used to decompose phenol, respectively.

ASSOCIATED CONTENT

Supporting Information

Reagents and materials, calculation of degradation rate constant k of photocatalysis, and EIS experiments. This material is available free of charge via the Internet at http://pubs.acs.org.

AUTHOR INFORMATION

Corresponding Authors

*E-mail: wangfeng0822@iccas.ac.cn. Address: P.O. Box 59, Institute of Chemistry, Chinese Academy of Sciences, Zhongguancun North First Street 2, Beijing, China 100190. Tel: +86-10-8261-2927. Fax: +86-10-8261-5665.

*E-mail: yms@iccas.ac.cn.

Author Contributions

The experiments were designed and carried out by P.L., F.W., S.Z., Y.D., J.Z., and M.Y. The manuscript was written by all authors. All authors have given approval to the final version of the manuscript.

Notes

The authors declare no competing financial interest.

■ ACKNOWLEDGMENTS

This work was supported by the National Basic Research Program of China (Grant 2012CB720300 and 2010CB933500) and National Natural Science Foundation of China (Grant 50973115 and 51133009). Special acknowledgment is given to Valentine Dolgov for his useful suggestions on editing the manuscript. Special acknowledgment is also given to Qing Li for her assistance with EIS measurements.

■ REFERENCES

(1) Fujishima, A.; Honda, K. *Nature* **1972**, *238*, 37−38.
(2) Fujishima, A.; Zhang, X.; Tryk, D. A. *Surf. Sci. Rep.* **2008**, *63*, 515−582.
(3) Xiong, Z.; Zhang, L. L.; Ma, J.; Zhao, X. S. *Chem. Commun.* **2010**, *46*, 6099−6101.
(4) Zhu, H.; Chen, X.; Zheng, Z.; Ke, X.; Jaatinen, E.; Zhao, J.; Guo, C.; Xie, T.; Wang, D. *Chem. Commun.* **2009**, *48*, 7524−7526.
(5) Reddy, K. R.; Nakata, K.; Ochiai, T.; Murakami, T.; Tryk, D. A.; Fujishima, A. *J. Nanosci. Nanotechnol.* **2010**, *10*, 7951−7957.
(6) Wang, D. S.; Zhang, J.; Luo, Q. Z.; Li, X. Y.; Duan, Y. D.; An, J. *J. Hazard. Mater.* **2009**, *169*, 546−550.
(7) Liang, H.; Li, X. *Appl. Catal. B: Environ.* **2009**, *86*, 8−17.
(8) Qiu, R.; Song, L.; Zhang, D.; Mo, Y.; Brewer, E.; Huang, X. *Int. J. Photoenergy* **2008**, No. 16472, 1−5.
(9) Zhang, M.; Chen, C.; Ma, W.; Zhao, J. *Angew. Chem., Int. Ed.* **2008**, *47*, 9730−9733.
(10) O'Regan, B.; Gratzel, M. *Nature* **1991**, *353*, 737−740.
(11) Wang, Y.; Zhong, M.; Chen, F.; Yang, J. *Appl. Catal. B: Environ.* **2009**, *90*, 249−254.
(12) Su, B.; Ma, Z.; Min, S.; She, S.; Wang, Z. *Mater. Sci. Eng., A* **2007**, *458*, 44−47.
(13) Kim, S. H.; Kwak, S.-Y.; Suzuki, T. *Polymer* **2006**, *47*, 3005−3016.
(14) Zhang, J.; Huang, Z. h.; Xu, Y.; Kang, F. Y. *New Carbon Mater.* **2011**, *26*, 63−70.
(15) Liu, Y.; Hu, Y.; Zhou, M. j.; Qian, H. s.; Hu, X. *Appl. Catal. B: Environ.* **2012**, *125*, 425−431.
(16) Yu, G.; Gao, J.; Hummelen, J. C.; Wudl, F.; Heeger, A. J. *Sicence* **1995**, *270*, 1789−1791.
(17) Di Paola, A.; Garcia-Lopez, E.; Marci, G.; Palmisano, L. *J. Hazard. Mater.* **2012**, *211−212*, 3−29.
(18) Lee, J.; Hong, J.; Park, D. W.; Shim, S. E. *Opt. Mater.* **2010**, *32*, 530−534.
(19) Li, H.-Y.; Chen, H.-Z.; Xu, W.-J.; Yuan, F.; Wang, J.-R.; Wang, M. *Colloids Surf., A* **2005**, *254*, 173−178.
(20) Wang, Y.; Kimura, K.; Dubin, P. L. *Macromolecules* **2000**, *33*, 3324−3331.
(21) Lei, P.; Wang, F.; Gao, X. W.; Ding, Y. F.; Zhang, S. M.; Zhao, J. C.; Liu, S. R.; Yang, M. S. *J. Hazard. Mater.* **2012**, *227−228*, 185−194.
(22) Gulgun, M. A.; Popoola, O. O.; Kriven, W. M. *J. Mater. Res.* **1995**, *10*, 1565−1570.
(23) Che, Y.; Datar, A.; Yang, X.; Naddo, T.; Zhao, J.; Zang, L. *J. Am. Chem. Soc.* **2007**, *129*, 6354−6355.
(24) Zhang, H.; Lv, X.; Li, Y.; Wang, Y.; Li, J. *ACS Nano* **2010**, *4*, 380−386.
(25) Li, L.-L.; Liu, K.-P.; Yang, G.-H.; Wang, C.-M.; Zhang, J.-R.; Zhu, J.-J. *Adv. Funct. Mater.* **2011**, *21*, 869−878.
(26) Chen, X. J.; Wang, Y. Y.; Zhou, J. J.; Wei, Y.; Li, X. H.; Zhu, J. J. *Anal. Chem.* **2008**, *80*, 2133−2140.
(27) Park, Y.; Singh, N. J.; Kim, K. S.; Tachikawa, T.; Majima, T.; Choi, W. *Chem.—Eur. J.* **2009**, *15*, 10843−10850.
(28) Xu, C.; Wei, X.; Ren, Z.; Wang, Y.; Xu, G.; Shen, G.; Han, G. S. *Mater. Lett.* **2009**, *63*, 2194−2197.
(29) Wang, Q.; Chen, C.; Zhao, D.; Ma, W.; Zhao, J. *Langmuir* **2008**, *24*, 7338−7345.
(30) Li, M.; Zhou, S.; Zhang, Y.; Chen, G.; Hong, Z. *Appl. Surf. Sci.* **2008**, *254*, 3762−3766.
(31) Kim, T. W.; Lee, M. J.; Shim, W. G.; Lee, J. W.; Kim, T. Y.; Lee, D. H.; Moon, H. *J. Mater. Sci.* **2008**, *43*, 6486−6494.
(32) Zhang, J.; Zhang, M.; Sun, R. Q.; Wang, X. *Angew. Chem., Int. Ed.* **2012**, *51*, 10145−9.
(33) Wang, D.-H.; Jia, L.; Wu, X.-L.; Lu, L.-Q.; Xu, A.-W. *Nanoscale* **2012**, *4*, 576−584.